

New technique for strengthening reinforced concrete beams with composite bonding steel plates

Su-hang Yang ^{1a}, Shuang-yin Cao ^{*1} and Rui-nan Gu ²

¹ School of Civil Engineering, Southeast University, Nanjing, Jiangsu, 210096, China

² Jiangsu Research Institute of Building Science CO., LTD., Nanjing, 210008, China

(Received December 10, 2014, Revised February 12, 2015, Accepted February 15, 2015)

Abstract. Composite bonding steel plate (CBSP) is a newly developed type of structure strengthened technique applicable to the existing RC beam. This composite structure is applicable to strengthening the existing beam bearing high load. The strengthened beam consists of two layers of epoxy bonding prestressed steel plates and the RC beam sandwiched in between. The bonding enclosed and prestressed U-shaped steel jackets are applied at the beam sides. This technique is adopted in case of structures with high longitudinal reinforcing bar ratio and impracticable unloading. The prestress can be generated on the strengthening steel plates and jackets by using the CBSP technique before loading. The test results of full-scale CBSP strengthened beams show that the strength and stiffness are enhanced without reduction of their ductility. It is demonstrated that the strain hysteresis effect can be effectively overcome after prestressing on the steel plates by using such technique. The applied plates and jackets can jointly behave together with the existing beam under the action of epoxy bonding and the mechanical anchorage of the steel jackets. The simplified formulas are proposed to calculate the prestress and the ultimate capacities of strengthened beams. The accuracy of formulas was verified with the experimental results.

Keywords: composite bonding steel plate; reinforced concrete beam; prestressed steel plates; u-shaped steel jackets; epoxy bonding; ultimate capacity

1. Introduction

It is realized that the stiffness, load capacity and ductility demand of the structure should be satisfied for RC rehabilitation, and the design method for this purpose should be simple and easy to use. High longitudinal reinforcing bar ratio of the existing structure strengthened with epoxy bonded steel plates or FRP can easily lead to over-reinforcement, especially for bridges, therefore, high strength is very important.

However, preloading including self-weight exists in practical structures. Concrete structures are usually strengthened under the preloaded states and the stress in laminates should be zero until further load is exerted, this implies that strain hysteresis in the laminates is later than that on the

*Corresponding author, Professor, E-mail: 101000873@seu.edu.cn

^a Ph.D. Student, E-mail: 835100403@qq.com

^b Professor, E-mail: yshjdrs@gmail.com

surface of concrete bonded, this phenomenon is called as strain hysteresis. The methods to tension the strengthening materials externally bonded to the tension face of the beam can partially offset the strain hysteresis induced by the high deadweight. The increasing quantity of the strengthening material in the beam bottom may results in over-reinforcement of RC beams. In case that the original reinforcing bars of the beam bottom fail to yield, the ductility and deformability of RC members would be significantly reduced.

The author has proposed the new technique for strengthening RC beams with CBSP consists of two layers of prestressed steel plates and the RC beam sandwiched, the enclosed U-shaped steel jackets are applied at the beam sides along the longitudinal direction at specified intervals and tightened with bolts at the beam top (see Fig. 1).

A full advantage of the mechanical behaviors of its two components of steel plate and concrete can be taken. On one hand, the prestressing on the strengthening steel plates and jackets can be generated with this CBSP technique before loading. The epoxy bonding precompressed steel plates are bonded in the compression zone at the top to act as the additional compression reinforcing bars, and the pretensioned steel plates are applied in the tensioned zone to act as the additional tensioned reinforcing bars at the bottom of the existing beam; On the other hand, the steel jackets act as the additional lateral stirrups of the RC beam. The bolts on the U-shaped jackets serve to apply the normal pressure and longitudinal friction force to the bottom steel plates which are bonded together with epoxy adhesive to restrain the steel plates from being separated, the debonding failure at the plate ends or at the jackets can be avoided (Bouazaoui *et al.* 2007). Besides, the prestressed steel plates and jackets can overcome the strain hysteresis induced from the dead-weight unloading. The steel-concrete-steel composite beam as shown can significantly improve the strength and stiffness of the CBSP rein-forced beam. This composite structure is applicable to strengthening the existing bearing high load.

This technique has the following specific advantages in comparison with other strengthening methods: (1) the steel plates and jackets only cause a slight increase in dimension and weight of the existing beam. (2) Before loading, the prestress exerted on steel plates and jackets can eliminate the affect of the stress strain hysteresis of the existing beam deduced from the preload. (3) The U-shaped steel jackets bonded at the beam sides can play a role of shear resistance and realize the reliable anchoring of the longitudinal steel plates to prevent shear failure from occurring before the flexural failure. (4) The sectional moment inertia is significantly improved by the longitudinal steel plates, while the bearing capacity and stiffness can be enhanced. The stiffness cannot be significantly improved for FRP strengthened beam, because of the thin thickness of FRP sheets. The strength and stiffness of FRP cannot be restored at a time; this has limited its application. (5) CBSP strengthened beam with steel plates at the top and bottom of the beam is equivalent to the

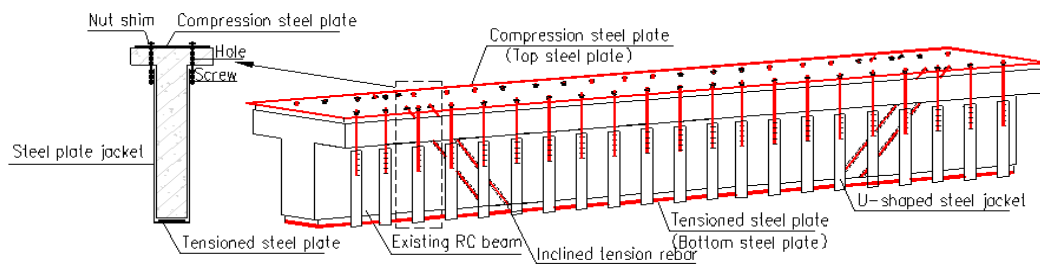


Fig. 1 RC beam strengthened with CBSP

double reinforced beam, so the problem in the over-reinforcement resulting from the strengthening materials applied only at the tensioned zone can be solved.

Over the past decades, different combinations of steel and concrete or masonry have been widely investigated, some of them concentrated on static Behaviors of Steel–concrete–steel Sandwich Beams (Xie *et al.* 2007), behavior of double skin composite construction (Mckinley *et al.* 2002), Flexural Behavior of Bonded Steel Concrete Composite Structures (Bouazaoui *et al.* 2007), CFT Columns with Horizontal Orthotropic Binding bars (Cai and Long 2007), Flexural Behavior of Steel plate-masonry Composite Beams (Jing *et al.* 2012, 2013), Fatigue Behavior of RC Beams Strengthened with Steel plate-concrete (Nie *et al.* 2011), and Shear Bearing Capacity of RC Short Column Retrofitted by Prestressed Steel Jackets (Priestley *et al.* 1994, Xiao and Wu 2003). Against the above background, the CBSP technique for a new combination of steel-concrete beam is proposed in this study to further investigate the design method, construction method and general procedure for strengthening RC beams. In order to testify if the technique can be used effectively in the RC beam rehabilitation, the real-scale RC beams strengthened with CBSP were tested and the mechanism and constructability were investigated.

2. Theory of CBSP technique

2.1 Affect of strain hysteresis

The external bonding of FRP and steel plate is affected by the strain hysteresis (Lam and Teng 2001, He *et al.* 2007) as depicted in Fig. 2(a). The initial load (such as deadweight) which can be hardly removed from the existing beam can result in the initial strain ε_{ini} on the beams. And the strain of the strengthening material is lagging behind that of the existing beam. The strain of the existing beam is ε_{ini} higher than that of the external bonding material. The stress of the external bonding material remains low until the longitudinal reinforcing bars are yielded. Such phenomenon is defined as stress strain hysteresis. The higher the strengthening material strength is, the more the hysteresis may be. Therefore, the material tensile strength cannot be fully utilized. It is noted that the strain hysteresis is not only found in the normal pure bending segment, but also in the shear span zone. The preloading effect should be considered in designs.

2.2 Effect of CBSP technique

The principle of the CBSP technique is illustrated in Fig. 2. The initial strain generated by the strengthening material can be equal to that of the bonded location with this technique. The affect of the strain hysteresis of the strengthening materials can be eliminated and the strength of the steel plates can be fully utilized. It can be achieved in two steps: (1) to calculate the initial strain ε_{ini} under the initial load on the bonded face of the strengthening materiel, since the initial stress strain hysteresis is various at all locations of the beam (see Fig. 2(a)); (2) to obtain the initial stress and strain of the steel plates equal to that of the bonded location in the beam by prestressing on steel plates. For the calculation of the ultimate bearing capacity of the strengthened beam, the corrected stress strain curve of the steel plates/jackets can be adopted (see Fig. 2(b)). The reinforcing bars in the existing beam fall in failure together with the strengthened steel plates/jackets.

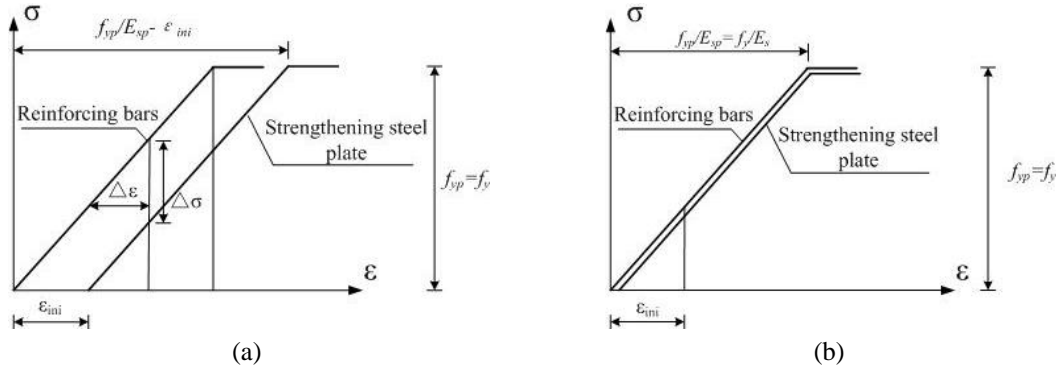


Fig. 2 Principle to overcome strain hysteresis

2.3 Calculation of ultimate capacity of CBSP-strengthened beams

2.3.1 Evaluation of flexural capacity

To evaluate the flexural capacity, the assumptions are made as follows: (1) the strains in strengthened beam vary linearly through the depth of the cross-section until the ultimate stage; (2) no slip is found at the interface between the concrete and the plates, no local buckling of the top steel plates occurs when the ultimate bending moment is reached; (3) no detrimental effect on the RC members is caused by the steel jackets.

The ultimate capacity of the CBSP strengthened beam can be expressed as the sum of the capacity of the existing beam and that of the additional flexural capacity resisted by the top and bottom steel plates of strengthened parts.

The ultimate flexural capacity M_u of CBSP subjected to bending can be expressed as the sum of the flexural capacities M_a resisted by the top and bottom steel plates of strengthened parts and beam M_o , as illustrated in Fig. 3. The flexural capacity of the existing beam M_o can be calculated according to codes ACI318, EN1992 and GB50010. The moment is taken based on the centre distance of the top plates and bottom plates, The area of the top steel plate is same as that of the bottom steel plates, the ultimate moment resistance is given by the flexural capacity of the strengthening steel plate M_a and can be calculated by Eq. (2).

$$M_u = M_o + M_a \quad (1)$$

$$M_a = F_{pt} \times h \quad (2)$$

$$F_{pt} = F_{pc} \quad (3)$$

$$F_{pt} = f_{ps} \times B_b \times T_b \quad (4)$$

$$F_{pc} = f_{ps} \times B_t \times T_t \quad (4)$$

Where f_{ps} is the tensile strength of the longitudinal steel plates; B_b , B_t are widths of bottom and top steel plates; T_b , T_t are thickness of bottom and top steel plates respectively; h is the height of the existing beam.

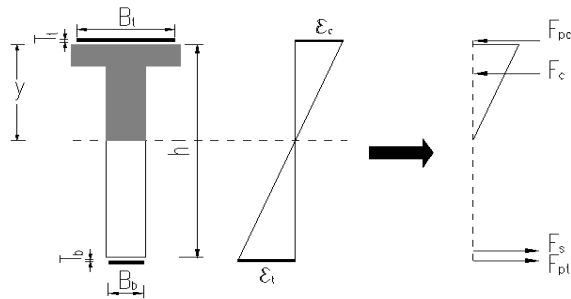


Fig. 3 Flexural calculation sketch for the strengthened beam

2.3.2 Evaluation of shear capacity

The shear resistant formulas are presented to prevent shear failure from occurring before bending failure. By reference to CEB-FIP specifications, the shear capacity is calculated using the method of the strut-and-tie model. The shear capacity of the strengthened beam V_u is derived from the sum of the tie direct action V_a and strut vertical action V_t , the calculation sketch is as shown in Fig. 4. For the calculation of the action of the vertical tie truss, the area of straight ties is the sum of the areas of plate jackets and stirrups within the effective range ($S = a/2$) of straight ties. Fig. 16 shows the relationship between r_{ds} and r_{vt} . The shear capacity V_u is calculated by Eq. (6).

$$V_u = V_a + V_t \tag{6}$$

$$V_t = A_s \times f_y + A_{gs} \times f_{gy} \tag{7}$$

$$V_a = \frac{r_{ds}}{r_{vt}} V_t \tag{8}$$

where A_s and A_{gs} are the areas of the stirrups and jackets within the effective range $S = a/2$ of straight strut acted by the vertical strut-and-tie truss, respectively. f_y and f_{gy} are the tensile strengths of stirrups and jackets, respectively. r_{ds} and r_{vt} are the distribution ratios of shear force directly applied by the straight strut and the vertical tie, as shown in Fig. 5.

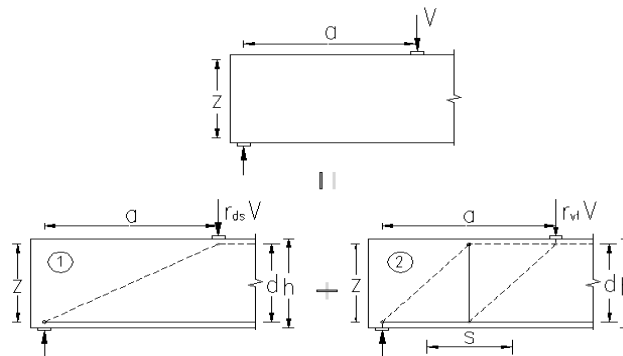


Fig. 4 Shear calculation sketch for the strengthened beam (Direct action of strut + action of vertical tie truss)

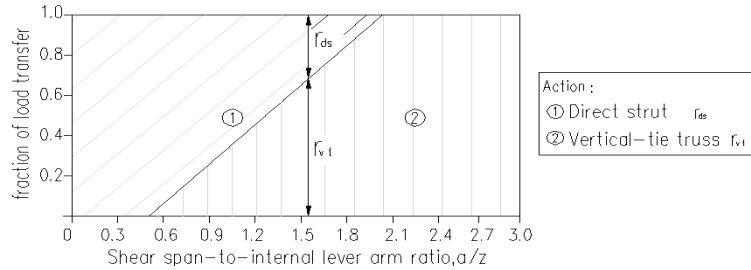


Fig. 5 Distribution ratios of shear forces (CEB-FIP Model Code 1990)

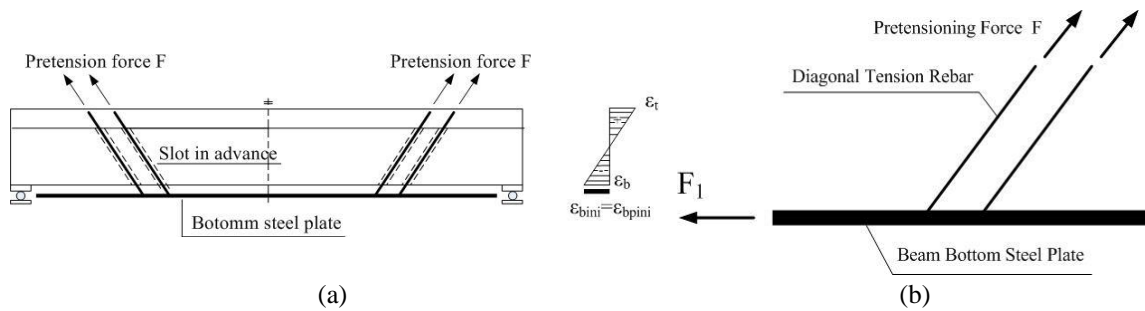


Fig. 6 Sketch of Pretension applied on bottom steel plate

2.4 Prestress calculation

2.4.1 Principle of pretension on bottom steel plate

The pretension is applied on the beam bottom steel plates as shown in Fig. 6. The pretension procedure is as follows. Slot at the beam sides, place the diagonally tensioned steel bars in slots. Weld the anchoring block on the bottom steel plate. Hold the plate by the diagonal rod at the position that the anchoring block is fixed as illustrated in Fig. 6(a). Tighten the rod through the beam flange at the beam top with nuts to apply pretension and create strain along with the bottom steel plate as illustrated in Fig. 6b. The initial strain in the bottom steel plate ϵ_{bpini} is calculated by Eq. (11).

$$F_1 = v_1 \cdot F \cdot \cos\theta \tag{9}$$

$$T_c = K \cdot F_1 \cdot d_1 \tag{10}$$

$$F = E_p \cdot \epsilon_{bpini} \cdot A_p \tag{11}$$

where F is the pretension force applied on the diagonal rod (N). v_1 is the reduction coefficient in consideration of the prestress loss of the steel plates, the value of the reduction coefficient v_1 is set to 0.9. F_1 is the pretension value established on the bottom steel plates (N). θ is the included angle between the horizontal lines of the diagonal rod and the beam bottom. T_c is the nut torque value (N·m). K is the torque coefficient, set to 0.12, in accordance with Reference (GB 50205 2001). d_1 is the diameter of the screws (mm). E_p is the elastic modulus of the steel plate. ϵ_{bpini} is the elastic strain of the bottom steel plate. A_p is the area of the bottom steel plate (mm^2).

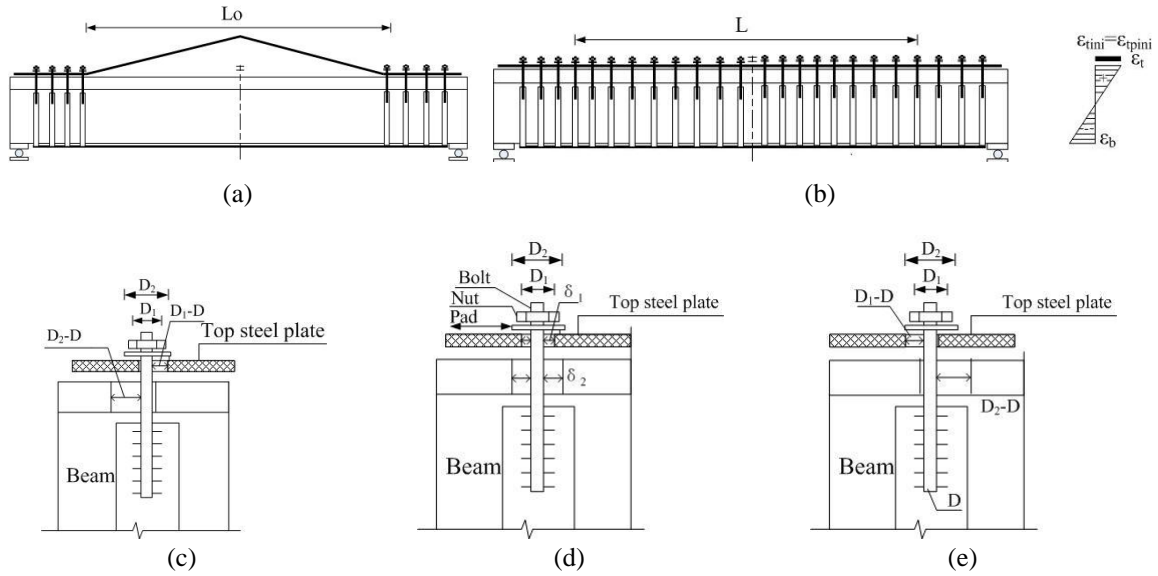


Fig. 7 Principle of Precompression applied on top beam steel plate

2.4.2 Principle of precompression applied on top beam steel plate

The precompression is applied on the beam top steel plate as shown in Fig. 7. The precompression is created by means of shortening the steel plate. Drill the bolt holes on the beam top steel plate in advance. The length of the top steel plate L_o is longer than the actual length of the beam bottom L . Install the plate jackets at both beam ends first, but do not firmly tighten (see Fig. 7(a)). Place the plate on the top of the beam and block it up so as to form the contact relationship between the steel plate and the bolt holes, the bolt holes and the holes on the beam flange as shown in Fig. 7. Then install the plate jackets from both sides to the middle and tighten them orderly to gradually even the top steel plate and eliminate the gap during compression of the beam top steel plate. The contact relationship between the steel plate and the bolt holes, the bolt holes and the beam flange holes is shown in Fig. 7. The initial strain in the top steel plate ϵ_{tpini} is calculated by Eq. (12).

$$\epsilon_{tpini} = v_2 \cdot (L_o - L)/L \quad (12)$$

$$L_1 = L_o + 2n \cdot (\delta_1 - \delta_2) \quad (13)$$

$$\delta_1 = (D_1 - D)/2 \quad (14)$$

$$\delta_2 = (D_2 - D)/2 \quad (15)$$

where ϵ_{tpini} is the elastic strain of the beam top steel plate. L_o is the calculated length of the top steel plate (mm). L is the length of the top steel plate deducting the length of the steel jackets installed at the two ends (mm). v_2 is the reduction coefficient considering the prestress loss of the steel plates, the reduction coefficient v_2 is set to 1.1. L_1 is the actual cutting length of the beam top steel plate (mm). n is the numbers of the preinstalled steel jackets. D is the diameter of the screw (mm). D_1 is

the diameter of the hole of the steel plate (mm). D_2 is the diameter of the hole of the beam flange (mm).

2.4.3 Principle of pretension applied on steel jacket

Fig. 8 shows the principle of pretension applied on steel jackets. The distribution of the shear stress on the shear span section of the beam is shown in Fig. 8 and calculated by Eq. (16). Tension the steel jacket to make the stress equal to the shear stress value of the beam section, thus the stress of the steel jacket is close to that of existing beam, see Eq. (19). Drive the screws welded on the jackets through the holes on the beam flange to form the enclosed steel jackets. Tighten the screws with the nuts to apply pretension on the jackets (see Fig. 5(a)). The stress applied on the jackets is calculated by Eq. (17).

$$\tau = V / b \cdot d_v \quad (16)$$

$$\sigma = F_2 / g_p \quad (17)$$

$$F_2 = K \cdot T_3 \cdot D \quad (18)$$

$$\tau = \sigma \quad (19)$$

$$\varepsilon_{jini} = \sigma / E_p \quad (20)$$

where τ is the shear stress in the shear span zone ($N \cdot mm^2$). V is the shear value in shear span zone (N). b is the width of the beam section (mm). d_v is the distance from the centroid of the beam bottom longitudinal reinforcing bars to that of the top of the beam (mm). σ is the tensile stress of the steel jacket ($N \cdot mm^2$). F_2 is the tension on the steel jacket (N). A_{gp} is the area of the steel jacket (mm^2), it is noted that the area of the steel plate jacket consists of the areas of its double limbs. E_p is the elastic modulus of the steel jacket (2.1×10^5 MPa). T_c is the nut torque value ($N \cdot m$). K is the torque coefficient, set to 0.12, in accordance with Reference (GB 50205 2001); ε_{jini} is the elastic strain of the steel jacket.

2.5 Calculation of initial stain ε_{ini} of the existing beam

The initial strain ε_{tini} and ε_{bini} at the tensioned and compressed edges of the existing beam that undergo preload on the pure bending segment can be calculated as follows with the uncracked and

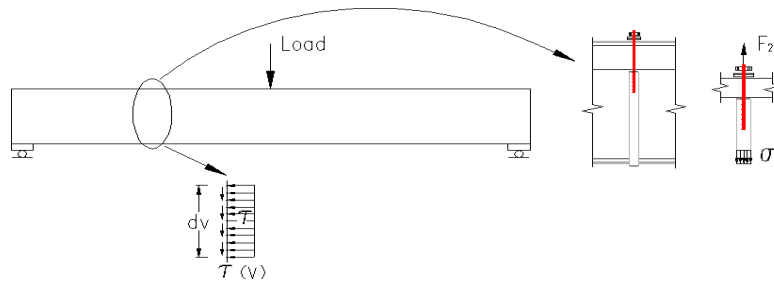


Fig. 8 Principle of pretension applied on steel jackets

cracked states taken into account. The formulas are derived from the section of the T-shaped beam. For the rectangular beam, the formulas are still applicable when h_f and b_f are zero.

2.5.1 Uncracked

For the uncracked state, convert the composite section into the concrete section. The height of the compressed section zone is

$$x_o = \frac{2a' \alpha_E A'_s + (b_f - b)h_f^2 + 2h_o \alpha_E A_s + h^2 - b}{2\alpha_E A'_s + 2(b_f - b)h_f + 2\alpha_E A_s + 2bh} \quad (21)$$

where b and h are the width and height of the beam. b_f is the flange width of the T-shaped beam, h_f is the flange height of the T-shaped beam. x_o is the theoretical height of the compressed zone. a' is the distance from the point of the resultant force of the compressed reinforcing bars to the compressed edge of the beam. A_s and A'_s are the areas of the tensioned reinforcing bars and the compressed reinforcing bars $\alpha_E = \frac{E_s}{E_c}$.

$$I_o = \frac{1}{3}bx_o^3 + \frac{1}{3}b(h - x_o)^3 + (\alpha_E - 1)A_s(h_o - x_o)^2 + (\alpha_E - 1)A'_s(x_o - a')^2 + \frac{1}{12}(b_f - b)h_f^3 + (b_f - b)h_f \left(x_o - \frac{h_f}{2}\right)^2 \quad (22)$$

where I_o is sectional moment of inertia in case of uncrack.

The initial tensile strain of the concrete at the beam tensioned edges can be given by Eq. (23).

$$\varepsilon_{bini} = \frac{M_o(h - x_o)}{0.85E_c I_o} \quad (23)$$

According to the plane section assumption, the initial compression strain of the concrete at the beam compressed edges can be given by Eq. (24).

$$\varepsilon_{tini} = \frac{M_o x_o}{0.85E_c I_o} \quad (24)$$

where M_o is the moment generated under the preloading. I_o is the moment of inertia on the cracking section. E_c is the concrete elastic modulus. E_s is reinforcing bars elastic modulus. ε_{bini} is the initial tensile strain of the bottom plates. ε_{tini} is the initial compression strain of the top plates.

2.5.2 Cracked

The tension is undertaken only by the bottom longitudinal reinforcing bars after cracking in the tensioned zone. To calculate the moment of inertia of the cracked section, the concrete in the compression zone is considered, but the concrete in the tensioned zone is ignored. The theoretical height of the compression zone x_o can be calculated by Eq. (25).

$$x_o^2 + \frac{2[\alpha_E A'_s + (b_f - b)h_f + \alpha_E A_s]x_o}{b} - \frac{2(\alpha' \alpha_E A'_s + h_o \alpha_E A_s)}{b} = 0 \quad (25)$$

$$I_1 = \frac{1}{3}bx_o^3 + \alpha_E A_s(h_o - x_o)^2 + (\alpha_E - 1)A'_s(x_o - a'_s)^2 + \frac{1}{12}(b_f - b)h_f^3 + (b_f - b)h_f\left(x_o - \frac{h_f}{2}\right)^2 \tag{26}$$

where I_1 is the moment of inertia on the cracking section.

The tensile strain of the concrete at the beam tensioned edges can be given by Eq. (27).

$$\varepsilon_{bini} = \frac{M_o(h - x_o)}{E_c I_1} \tag{27}$$

The initial tensile strain of the concrete at the beam compressed edges can be given by Eq. (28).

$$\varepsilon_{tini} = \frac{M_o x_o}{E_c I_1} \tag{28}$$

where M_o is moment generated under the preloading. I_1 is the moment of inertia on the cracking section. E_c is concrete elastic modulus. E_s is reinforcing bars elastic modulus. ε_{bini} is the initial tensile strain of the bottom plates. ε_{tini} is the initial tensile strain of the top plates.

2.6 Calculation for CBSP strengthening

- (1) With the consideration of the actual status and loading, calculate the initial strain by Eqs. (23), (24), (25) and (28) (see Fig. 9(a)).
- (2) Calculate the prestress applied on the beam bottom steel plate by Eq. (12), make such prestress equal to that calculated by the Eq. (23) or Eq. (27), and apply the prestress on the bottom steel plate as per the method mentioned in this paper (see Fig. 9(b)).
- (3) Calculate the prestress applied on the beam top steel plate by Eq. (12), make such prestress equal to that calculated by the Eq. (23) or Eq. (28), and apply the prestress on the top steel plates as per the method mentioned in this paper (see Fig. 9(c)).

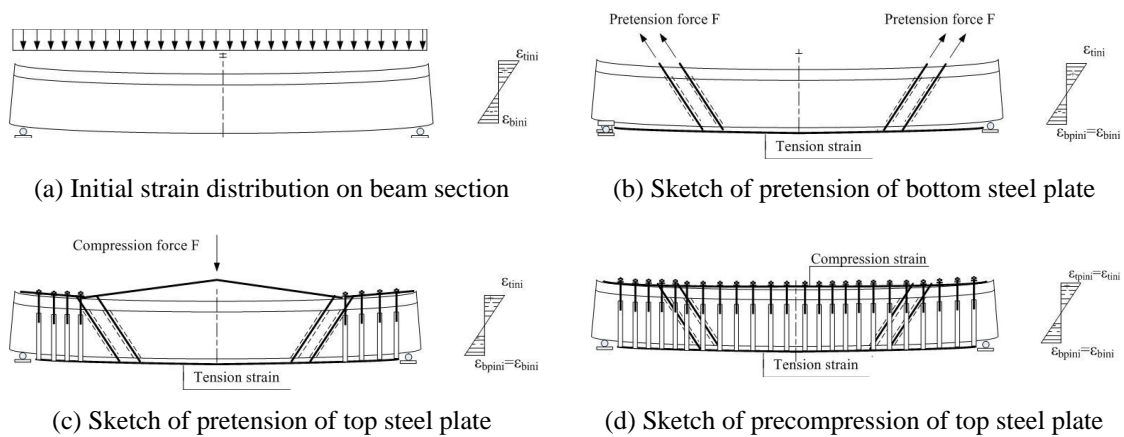


Fig. 9 Schematic of pretension of steel plate

- (4) Calculate the prestress applied on the steel jacket by Eq. (17), and apply the prestress on the steel jackets as per the method mentioned in this paper (see Fig. 9(d)).

3. Experimental procedure of CBSP-strengthened beam

3.1 Specimen design

Four full-scale RC T-shaped beams were prepared according to the actual sizes of bridge in the practical engineering. Three of them were strengthened with CBSP and one was used as the comparison beam. The geometrical dimensions of those four existing beams in the tests are same, with a total length of 5950 mm, the clear span of 5750 mm between two supporting points and the height of 1200 mm. The details and sizes of the specimens are shown in Fig. 10.

3.2 Material properties and specimen construction

The compressive strength of concrete cubes cured in average standard 28 days is approximately 45.0 MPa as shown in Table 1, the concrete elastic modulus E_c is 32,500. The reinforcing bars with diameter of 25 mm, 14 mm and 10 mm are used as longitudinal reinforcing bars, stirrups with the diameter of 12 mm are used. The thickness of U-shaped jackets is 4.0 mm and the width is 50.0 mm, the screws at both ends are made of $\Phi 14.0$ mm round steel. The centre distance of the steel jackets between the loading points within the length of 1900 mm is 300.0 mm, 200.0 mm in

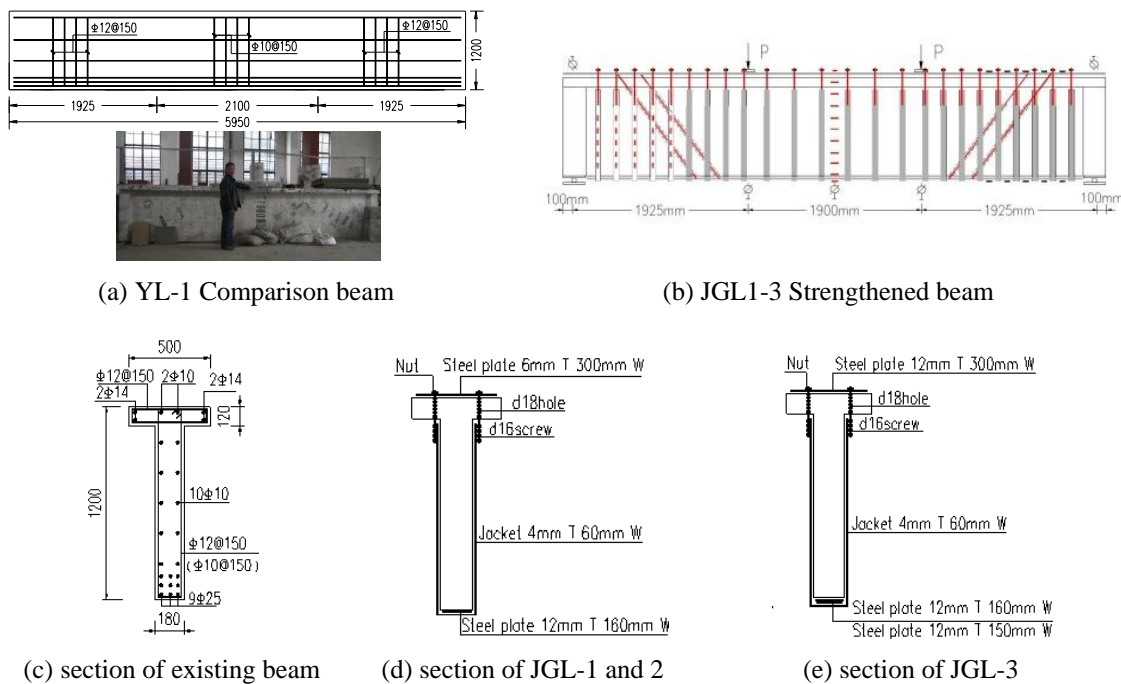


Fig. 10 Details of specimens (mm)

Table 1 Details and sizes of specimens

CBSP beam	State before strengthening	Thickness of steel plates (mm)	Ratio of the bolt spacing at the top to the plate thickness (s/t)	Concrete compressive strength (MPa)
YL1	Undamaged	/	/	49.2
JGL1	Undamaged	Top plate: 6 mm thick, 300 mm wide. Bottom plate: 12 mm thick, 170 mm wide.	50.0 (between loading points) 33.3 (at the other places)	47.6
JGL2	Flexural failure	Top plate: 6 mm thick, 300 mm wide. Bottom plate: 12 mm, thick 170 mm wide.	50.0 (between loading points) 33.3 (at the other places)	51.3
JGL3	Undamaged	Top plate: 12 mm thick, 300 mm wide. Bottom plate: 6 mm thick, 160 mm wide(the first layer) 6 mm thick, 150 mm wide (the second layer)	25.0 (between loading points) 16.7 (at the other places)	45.2

Table 2 Material properties of steel plates and reinforcing bars

Properties	Steel plates				Steel reinforcing bars			
	4.0 mm	6.0 mm	12.0 mm	$D=10.0$ mm	$D=12.0$ mm	$D=14.0$ mm	$D=16.0$ mm	$D=25.0$ mm
Yield strength (MPa)	242.3	359.3	339.3	372.2	368.5	353.6	236.1	339.2
Ultimate strength (MPa)	420.6	582.4	550.3	589.4	575.9	572.2	443.7	554.6
Elastic modulus (E_p/E_s)	200,000	200,000	200,000	210,000	210,000	210,000	210,000	210,000

the rest sections. The thickness of longitudinal steel plate is 6.0mm or 12mm. The diagonal ties are made of reinforcing bars with the diameter of 16 mm (round steel). The details and dimensions of specimens are listed in Table 1. The compressive strength of epoxy adhesive is 49.0 MPa. The mechanical properties of the materials were determined in the test, the test data are shown in Table 2.

Those specimens are prepared according to the steps described previously. The preload is considered as the deadweight of the existing beam. Four steel jackets are mounted at each end first in the fourth step of the installation of the beam top steel plates. In Eq. (13), n is taken as 4. The diameter of the bolt is 16.0 mm, the diameter of the bolt holes on the steel plates is 18.0 mm, and thus δ_1 is 1.0 mm. The diameter of the bolt holes on the beam flange is 18.0 mm, thus δ_2 is 1.0 mm.

3.3 Test setup and instrumentation

The specimens were tested at the four-point bending with the setup shown in Fig. 11. The tests



Fig. 11 Test setup for CBSP-strengthened beam

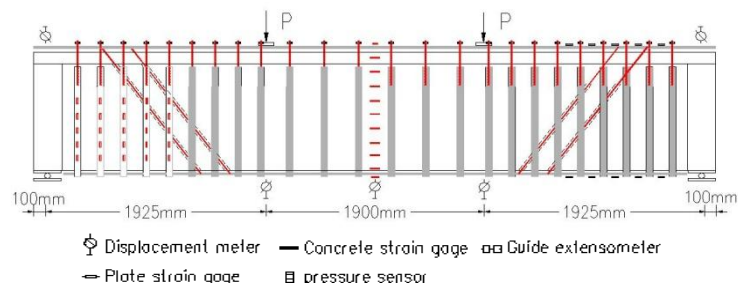


Fig. 12 Specimen test scheme

were conducted using two hydraulic jacks with the capacity of 320-ton in the structural laboratory. The measurement instruments including two load cells to measure the applied load, three linear variable differential transformers (LVDT) were adopted to detect the midspan and loading point deflection of each beam; numerous strain gauges were bonded on the surfaces of the steel plates /jackets and concrete to detect the strain development. The locations of all the test points are shown in Fig. 12.

3.4 Test procedure

Before the formal loading, an initial load of 5% of expected peak load (based on a theoretical calculation) was applied to ensure the good working performance of the mechanical and electronic equipment. The load was then released and all the readings were returned to zero. Loading was applied to each beam in increments of approximately 5% of the expected peak load. After each loading, wait for five minutes to ensure that the deformation of the beam occurs no longer. Continue loading until the beam broken in failure.

4. Test results and discussion

4.1 Prestress efficiency of steel plates and jackets

During the preparation of specimens, the accuracy of the prestress applied on steel plates/jackets and calculated by the method presented in this paper was testified. The theoretical values in

Table 3 Experiment on prestresses applied on steel plates and jackets

CBSP Beams	Beam top steel plate			Beam bottom steel plate			Steel jacket		
	Theoretical value (ε_{ini})/10 ⁻⁶	Tested value (ε_t)/10 ⁻⁶	$\varepsilon_{ini}/\varepsilon_t$	Theoretical value (ε_{bini})/10 ⁻⁶	Tested value (ε_t)/10 ⁻⁶	$\varepsilon_{bini}/\varepsilon_t$	Theoretical value (ε_j)/10 ⁻⁶	Tested value (ε_t)/10 ⁻⁶	$\varepsilon_j/\varepsilon_t$
JGL-1	2	4	0.5	12	14	0.857	280	312	0.897
JGL-3	2	3	0.667	14	16	0.875	280	296	0.946

Table 3 are the initial strains of the bonded locations created by deadweight, and the strain hysteresis can be overcome by the prestress exerted on the steel plates of the midspan section and jackets. The tested values are the prestresses applied on the steel plates measured by the strain gauges. The prestress applied on the side steel jackets is calculated by the average value read on the strain gage on the plate jackets. It can be seen from Table 3 that the test results are in good agreement with that of the theoretical calculation. The error between the test values and the theoretically calculated value is not over 10%. The prestress exerted on the steel plates might be influenced by the structural adhesive coated on the steel plates/jackets, and the steel jackets were still in elastic state due to the structural adhesive not yet solidified, the formulas of the prestress applied on the steel plates and jackets were proven to be accurate and feasible, with the consideration of the appropriate reduction coefficient.

4.2 Failure mode of CBSP strengthened beam

Fig. 14 shows the cracking distribution at failure observed during the test. The following characteristics of cracking distribution are observed:

- (1) JGL1 is failed in the flexural failure mode, the maximum width of the crack at the pure bending segment is greater than 2.0 mm, and the width of the diagonal crack at shear span segment is much smaller (see Fig. 14(b)). Cracks of JGL1 are more intensive than that of YL1 (see Fig. 14(a)), but the width and space become smaller along with the height extending upwards the top of the beam.
- (2) The failure mode of JGL2 is similar to that of JGL1, the maximum width of cracks at several positions of the pure bending segment at failure is 2 mm (see Fig. 14(c)). It can be assumed that both the bottom steel plates and tensioned longitudinal reinforcing bars were yielded.
- (3) Diagonal cracks appear on the shear span segment of JGL1, JGL2, but the width of the diagonal crack is not over 0.4 mm till the beam bended in failure, and the maximum width is found only when the beam is coming close to failure.
- (4) JGL3 is failed in shear; the width of the diagonal cracking at the shear span segment at failure is greater than 2 mm (see Fig. 14(d)). Only slight slip is observed on jacket-concrete interface. It also means that the steel jackets and stirrups were yielded at the positions with the maximum diagonal crack. The cracks at the shear span segment of JGL3 are more intensive than that of JGL1 and more fully developed, the maximum width of the diagonal crack in failure is greater than 2.0 mm, and the width of the crack at the normal section is less than 0.4 mm.

- (5) Debonding is not found at the steel-concrete interface at the beam bottom. No local buckling is observed on the top steel plate. The integrity is shown in Fig. 13.
- (6) The noise to separate the bottom steel plate or steel jackets from the beam could be heard at the last loading stage.

The local buckling is not observed on the top of the beam. Because the top steel plate is subjected to the constraints of binding bolts and epoxy bonding, the mechanism is similar to those observed in concrete-filled tubular column (Cai and Long 2007). Table 1 indicates that when the value of s/t is smaller than 50, no local buckling at the ultimate load could occur. But the future axial load tests for the local buckling performance of the top steel plates are still necessary to investigate the appropriate ratios of binding bolt spacing to the steel plate thickness.

No debonding occurs on the bottom steel plates, the enclosed U-shape steel jackets can play a role of the additional anchors for the beam bottom steel plates to avoid the debonding failure at the plate ends or between the jackets. The failure mode of strengthened beam is the overall flexure or shear failure mode, similar to that of RC members. This is useful for more sophisticated FE analysis of CBSP-strengthened RC beams.

Note: figures in () are the cracking loads at the shear span segment, the cracking load of JGL2 is the re-cracking load after repair. P_{cr} is the load in case of cracking; P_y is the tested load of the corresponding midspan in case of plate being yielded. P_u is the tested maximum load born by the test members. δ_y and δ_u are tested midspan deflections corresponding to P_y and P_u . BM indicates the flexural failure mode; SM indicates the shear failure mode.

Table 4 Principal test results

CBSP beams	Cracking load P_{cr}/kN	Yield load P_y/kN	Ultimate load P_u/kN	δ_y (mm)	δ_u (mm)	P_u/P_{cr}	P_u/P_y	$\mu = \delta_u/\delta_y$	Failure mode
YL1	125(185)	800	950	10.33	15.21	7.6	1.18	1.48	BM
JGL1	325(550)	1300	1400	13.22	19.43	4.31	1.03	1.47	BM
JGL2	185(200)	750	900	15.8	25.2	7.82	—	1.59	BM
JGL3	775(450)	—	1860	—	20.08	—	—	—	SM



(a) Top steel plate



(b) Bottom steel plate

Fig. 13 Unbroken top and bottom steel plates

4.3 Ductility

The displacement ductility index μ is defined as the ratio of the ultimate displacement δ_u to the yield displacement δ_y ($\mu = \delta_u / \delta_y$) shown in Table 4. It could be found that the ductility of JGL1, JGL2 failed in flexure is almost same as that of the existing beam. The failure behavior of the beam failed in flexure can be considered ductile. This is because the existing beam reinforcing bars are yielded, so the ductility demand of the strengthened beam can be satisfied due to the deformation and yielding of the tensile reinforcing bars.

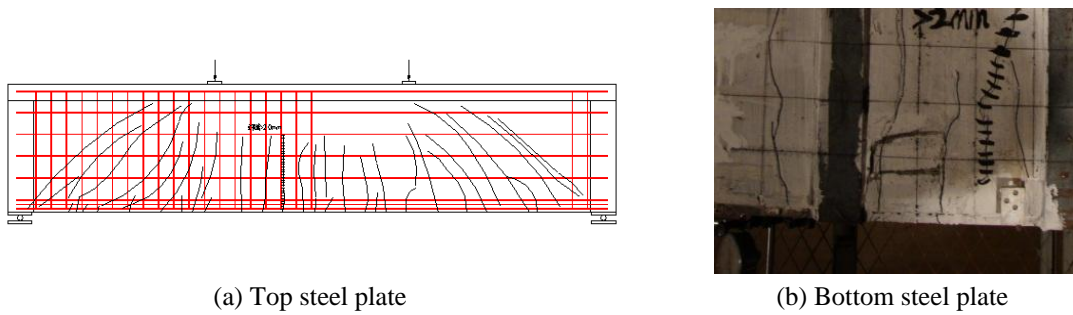


Fig. 14 Unbroken top and bottom steel plates

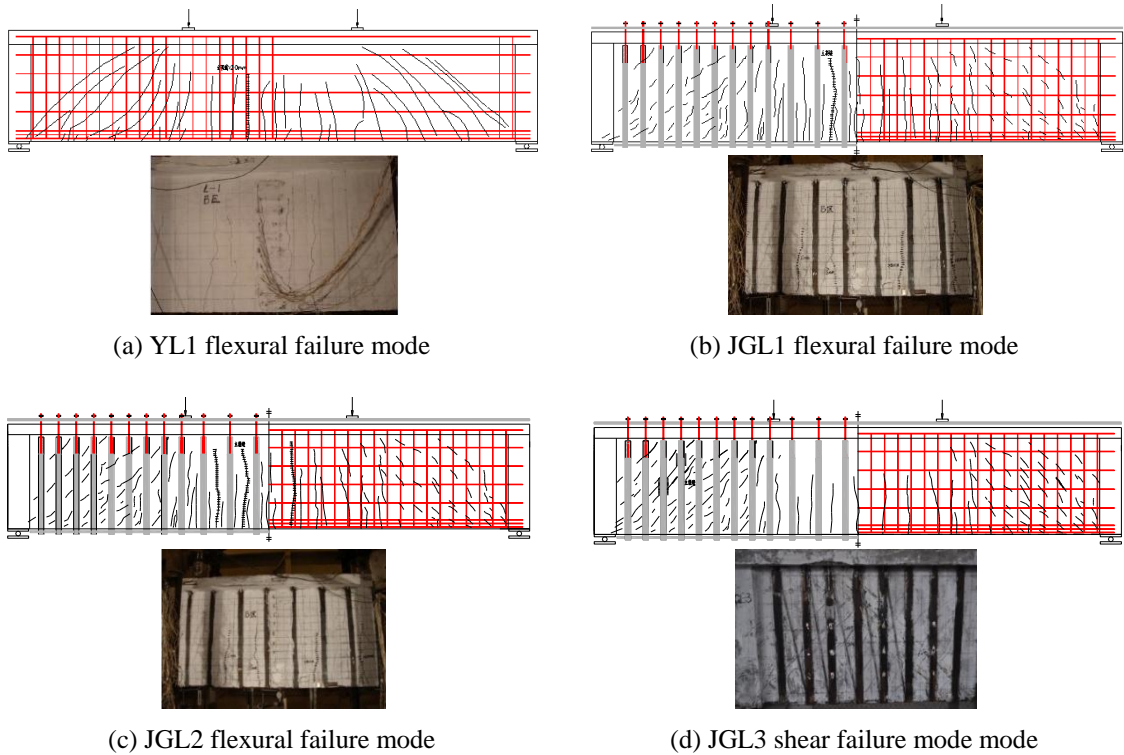


Fig. 15 Crack distribution and failure of specimen

Table 5 Comparison between calculated and tested loads

CBSP beams	Calculated value $P_{u,ca}$ (kN)	Tested value $P_{u,t}$ (kN)	$P_{u,ca}/P_{u,t}$
JGL1	1320	1400	0.94
JGL2	790	850	0.92
JGL3	1550	1860	0.86

4.4 Ultimate capacity of the CBSP-strengthened beam

The ultimate loads of all the specimens are given in Tab.4. The increase in cracking load of the normal section for JGL1 is 160%, the increase in ultimate load is 47%. The increases in cracking load of the diagonal section and in ultimate load for JGL3 are 220% and 95%, respectively. The ultimate load for JGL2 is restored to state before the failure of the comparison beam occurs.

The ultimate capacity of the strengthened beams calculated by the formulas in this paper is given in the Table 5. The flexural capacity of the existing beam M_o is calculated according to codes GB50010. It indicates that the proposed method can sufficiently meet the design requirements for strengthened beams. The ultimate capacity of the strengthened beam can be expressed as the sum of the capacity of the existing beam and the additional flexural capacity resisted by the top and bottom steel plates of strengthened parts. The maximum capacity can be improved since the debonding failure of strengthened parts is avoided.

4.5 Load-displacement behavior response

The curves of the applied load versus displacement are shown in Fig. 15. It can be observed that the curve of JGL1 is approximately in linear at the early loading stage. The slope of the curve is gradually decreased; this marks the beginning of the non-linear stage after cracking. By comparison of JGL1 with YL1, the initial increase of the slope indicates an improvement in the flexural stiffness of JGL1. The decrease in the curve slope in great extent marks the beginning of the yielding of the bottom steel plates and reinforcing bars.

Compared with FRP for strengthening, the area of the steel plates is larger, the inertia moment of the strengthened beam section is obviously bigger, and the increase in the stiffness is more significant. Although the shear failure occurs in JGL3, the midspan deflection is still less than that of JGL1. The flexural capacity of the JGL2 is restored to the level of YL1. But its flexural stiffness is not restored to the level of YL1.

Based on the investigation in this paper, the service load of the beam is up to 90% of the ultimate load. Fig. 15 shows that the deflection of all the beams at the service limit is nearly in linear; the flexural stiffness can be compared with the inertia moments of the beam section. The inertia moment I_1 of YL1 can be calculated by Eq. (23). And the inertia moment of I_2 of JGL2 can be calculated on the basis of the horizontal centroid axis x_o of the cracking existing beam, which is taken as that of the combined sections. The inertia moment of the JGL2 is the sum of that of the top and bottom steel plates and calculated relative to the centroid axis x_o , ignoring the concrete core. The area of the steel plate can be inverted into that of the concrete and multiplied by the ratio of the steel plate elastic modulus to that of the concrete ($\alpha E = E_s/E_c$). The ratio of inertia moment of I_1 to that of I_2 is 1.818:1.0, the ratio of the service limit state deflection of YL1 to that of JGL2 is about 1.633:1.0. It is indicated that the analysis on the deflection of JGL2 is reasonable.

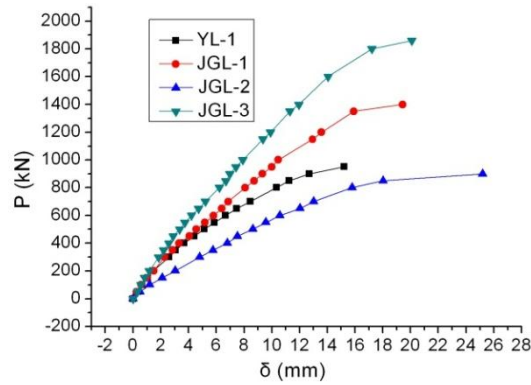


Fig. 16 Curves of midspan load versus displacement of specimen

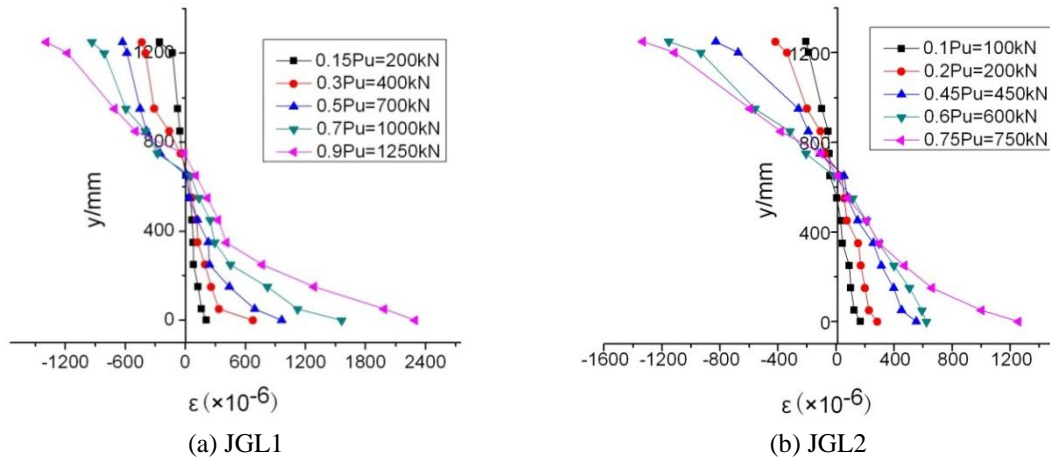


Fig. 17 Distribution of strain of midspan section

4.6 Strain distribution of CBSP strengthened beam along the beam depth

The strain distributions of the steel plates in the midspan along the depth of beams JGL1, JGL2 are plotted in Fig. 16 respectively. The ordinate y in the Fig. 16 represents the height along the cross-section. $y = 0$ is the level of the beam bottom steel plate. $y = 1200$ mm is the level of the beam top steel plate. Fig. 16 shows that the strain distribution along the beam depth in the cross-section of the midspan is nearly in linear, so it is verified that the assumptions of plane section are reasonable for the strengthened beam. It can be proved that no evident local buckling for the top steel plate and no bond-slip for the bottom steel plate are found in the midspan section.

4.7 Effectiveness of CBSP-strengthened beam

The curves of the applied load versus the strain of bottom steel plate and reinforcing bars of JGL1 midspan section are shown in Fig. 17. It can be seen that the increase in strain of the reinforcing bars is basically same as that of the steel plate and it is clear that the steel plates can

undertake the load of the strengthened beam promptly with the reinforcing bars of the existing beam. After cracking, the strain of the reinforcing bars grew almost in step with that of the steel plate which can fully share the stress of the reinforcing bars.

When the ultimate capacity of the strengthened beam is reached, its strain grows more rapidly than that in the reinforcing bars. The maximum strain of the reinforcing bars is $5,132 \times 10^{-6}$, the maximum strain of the steel plate is $9,256 \times 10^{-6}$, it indicates that both reinforcing bars and steel plates were yielded. This is because the steel plate is further away from neutral axis than the reinforcing bars.

The curves of the applied load versus the strain of the top steel plate and concrete of midspan section for JGL1 are shown in Fig. 18. It shows that the strain of the beam top steel plate grows almost in step with that of the concrete before JGL1 beam cracking. After cracking, the increase in strains of the steel plate remains slight greater than that of the concrete until the beam falls in failure. It is noted that the steel plate strain is always greater than the concrete strain. This is also because the top steel plates are further away from the neutral axis than the compressed concrete. The maximum strain of the steel plate is $1,483 \times 10^{-6}$, and this means the top steel plates yielding.

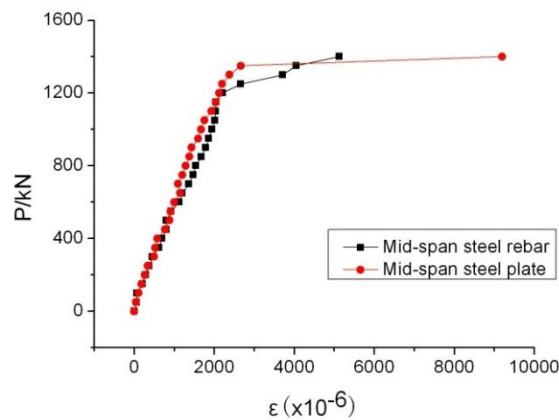


Fig. 18 Load-strain curve of midspan section of bottom steel plate and reinforcing bars for JGL1

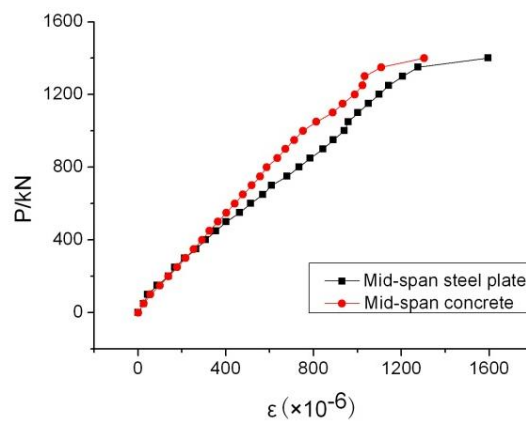


Fig. 19 Load-strain curve of midspan section of top steel plate and concrete for JGL1

The curves of the applied load versus the strain of steel jackets and stirrups for JGL1 are shown in Fig. 19. It shows that the strain of the steel jackets grows rapidly after cracking of the diagonal section of JGL1 and is slightly greater than the strain in the stirrups. The increasing in strains for stirrups and steel jackets is kept in step when they are coming close to failure. The steel plates and jackets also fall in yielding in step.

The test results indicate that the strain hysteresis effect can be effectively overcome after prestressing the steel plates with the method presented in this paper. Under the action of the epoxy bonding and the mechanical anchorage of the steel jackets, the applied plates/jackets can jointly share the loads with the existing beam. The steel plates can play the same role as the reinforcing bars in the beam. Meantime, the externally bonded plate jackets can act the same function as the stirrups.

The strain distribution along axial direction of the top steel plates of strengthened beam JGL1, JGL2 are shown in Fig. 20. The x-axis represents the distance from the midspan to the support, $x = 0$ is the midspan position. The shear stress at the interface between the beam top steel plates and concrete can be calculated according to Fig. 20. The existing research has shown that the

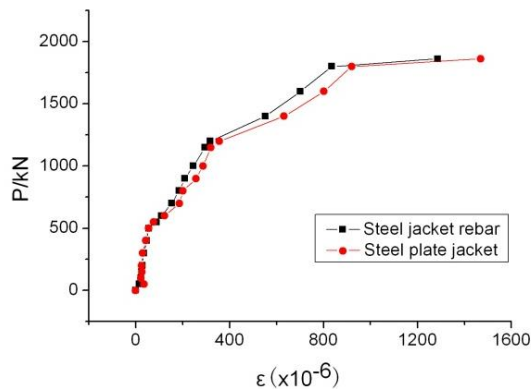


Fig. 20 Load-strain curve of plate jacket and stirrup
(The fourth steel jacket from the left, the forth strain gauge from the bottom)

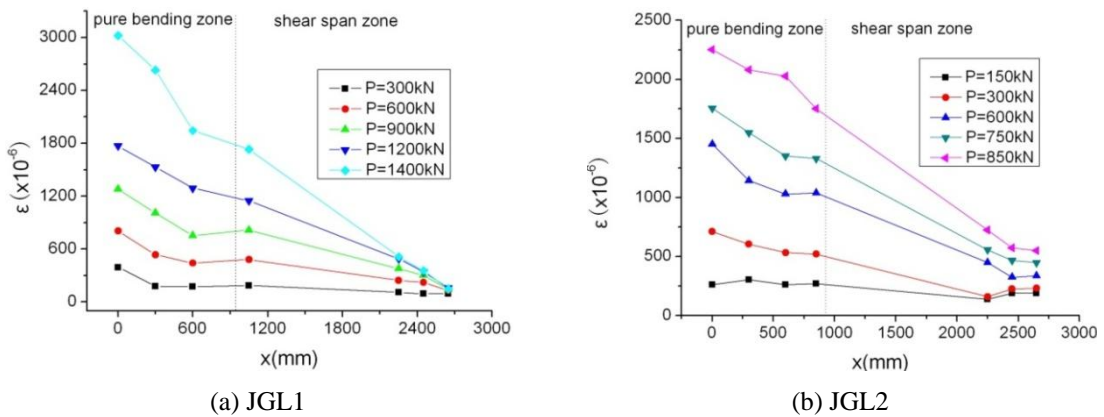


Fig. 21 Strain distribution along axial direction of top steel plate of CBSP strengthened beam

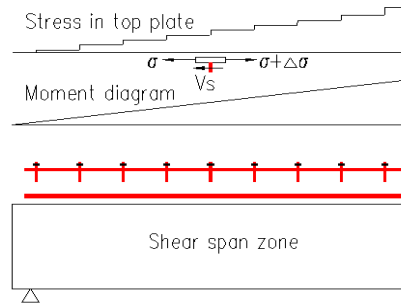


Fig. 22 Relationship of bending moment distribution in shear span segment versus strain of beam top steel plate

interfacial shear stress in such steel-concrete interface consists of two components as follows (Nie 2011): (1) compression stress difference produced due to the bending moment changing along the shear span segment, the shear force balance on the interface is needed (see Fig. 21); (2) the interface shear force produced by the shear force of the shear span segment. It is clear in the Fig. 20 that the strains of the top steel plate in the shear-span segment are distributed linearly and decreased gradually in the axial direction towards the beam support ends. But the plate strain would not attenuate to zero even on the supporting positions of the ends; the existence of the second effect is proved. The interface shear force caused by the two kinds of effects should be taken into account in the strength design for the top steel-concrete interface.

5. Conclusions

The CBSP strengthening technique is introduced in this paper. Based on the above concept analyses, test results and discussion, the following conclusions can be drawn.

- (1) The strengthening for RC beam with the new CBSP technique is successful. It is demonstrated from the test results that the failure modes of the CBSP-strengthened beams include the overall flexure mode or shear failure mode and yielding failure mode of the steel plate or jacket, the steel-concrete interface is kept in good condition, the steel plate and jacket can work well together with the existing beam.
- (2) The cracking load, stiffness, yielding load and maximum capacity of RC beams can be significantly improved with CBSP strengthening. The cracking load and capacity of the strengthened beam can be increased by 220% and 95%, respectively. The stiffness of the members can be enhanced, without evident reduction of the flexural ductility.
- (3) The assumptions of the plane section are acceptable for the strengthened beam. The flexural failure of the strengthened beam can be turned into the shear failure due to the increasing quantity of the longitudinal steel plates. Therefore, it is necessary to prevent such flexural failure occurring before the shear failure. The simplified design formulas are proposed for calculating the flexural and shear ultimate capacities of strengthened beams, and the values given by the formulas were verified with the experimental results. The proposed formulas were validated with test results and can be used to accurately calculate the capacities of the normal beams and the beams failed in prebending.
- (4) The prestressed steel plates can share the load promptly with the existing beam. The strain

hysteresis existing in strengthening structure can be eliminated; the strength of the steel plates can be fully utilized. The simplified formulas to calculate the prestress of strengthened beams are proposed, the results obtained using the method presented in this paper are in good agreement with the test results.

- (5) The stresses on the top beam plate distribute linearly to prove that the steel plates can effectively work together with the concrete after bolting and adhesive bonding. The steel plates can play the same role as the reinforcing bars in the beam. Meantime, the externally bonded plate jackets can act the same function as the stirrups.
- (6) When the value of s/t is less than 50, no local buckling at the ultimate load is found in this test. To avoid the local buckling, debonding and brittle failures of the steel plates of the strengthened beam, the details on the bottom beam steel-concrete interface with the anchored jackets should be further investigated.

Acknowledgments

The experimental part of this research was sponsored by department of science and technology of Jiangsu Province. The author gratefully acknowledges the support provided by the sponsor.

References

- ACI Committee 318 (2008), Building Code Requirements for Structural Concrete (ACI 318-08) and Commentary, American Concrete Institute, Farmington Hills, MI, USA.
- Bouazaoui, L., Perrenot, G., Delmas, Y. and Li, A. (2007), "Experimental study of bonded steel concrete composite structures", *J. Construct. Steel Res.*, **63**, 1268-1278.
- Cai, J. and Long, Y.L. (2007), "Axial load behavior of rectangular CFT stub columns with binding bars", *Adv. Struct. Eng.*, **10**(5), 551-565.
- CEB-FIP Model Code (1990), Thomas Telford services, Ltd., London, UK, (1993), 437.
- European Committee for Standardization (2004), Eurocode 2: Design of concrete structures, Part 1: General rules and rules for buildings.
- GB 50010 (2010), Code for Design of Concrete Structures; China Architecture & Building Press, Beijing, China.
- GB 50205 (2001), Code for acceptance of construction quality of steel structures; China Architecture & Building Press, Beijing, China.
- He, X.J., Zhou, C.Y., Li, Y.H. and Xu, L. (2007), "Lagged strain of laminates in RC beams strengthened with fiber-reinforced polymer", *J. Central South Univ. Technol.*, **14**(3), 430-435.
- Jing, D.H., Cao, S.Y. and Shi, L. (2012), "Flexural behavior of steel plate-masonry composite beams", *Steel Compos. Struct., Int. J.*, **13**(2), 123-137.
- Jing, D.H., Pan, Y.X. and Chen, Y.L. (2013), "Axial behavior of MFT stub columns with binding bolts and epoxy adhesive", *J. Construct. Steel Res.*, **86**(2), 115-127.
- Lam, L. and Teng, J. (2001), "Strength of RC cantilever slabs bonded with GFRP strips", *J. Compos. Construct.*, **5**(4), 221-227.
- McKinley, B and Boswell, L.F. (2002), "Behaviour of double skin composite construction", *J. Construct. Steel Res.*, **58**(10), 1347-1359.
- Nie, J.G. (2011), *Steel-Concrete Composite Bridges*, China Architecture Building press, Beijing, China.
- Nie, J., Wang, Y. and Cai, C.S. (2011), "Experimental research on fatigue behavior of RC beams strengthened with steel plate-concrete composite technique", *J. Struct. Eng.*, **137**(7), 772-781.
- Priestley, M.J.N., Seible, F. and Xiao, Y. (1994), "Steel jacket retrofitting of reinforced concrete bridge

- columns for enhanced shear strength – Part 2: Test results and comparison with theory”, *ACI Struct. J.*, **91**(5), 537-551.
- Wright, H.D., Oduyemi, T.O.S. and Evans, H.R. (1991), “The experimental behavior of double-skin composite elements”, *J. Construct. Steel Res.*, **19**(2), 97-110.
- Wu, Y.F., Yan, J.H., Zhou, Y.W. and Xiao, Y. (2010), “Ultimate strength of reinforced concrete beams”, *ACI Struct. J.*, **107**(4), 451-462.
- Xiao, Y. and Wu, H. (2003), “Retrofit of reinforced concrete column using partially stiffened steel jackets”, *J. Struct. Eng.*, **129**(6), 725-732.
- Xie, M., Foundoukosb, N. and Chapmanb, J.C. (2007), “Static tests on steel–concrete–steel sandwich beams”, *J. Construct. Steel Res.*, **63**(6), 735-750.

CC